

# Aerosol dynamics in a turbulent flow

## Y. Wang\*

Division of Oil and Gas Resource, Institute of Geology and Geophysics, Chinese Academy of Sciences, P.O. Box 9825, Beijing 100029, PR China

Received 27 July 2007; received in revised form 15 November 2007; accepted 16 November 2007

### Abstract

The dynamics of aerosols in a turbulent flow is studied. The aerosol motion is described by the Langevin equation. The aerosol size distribution is calculated by the Fokker-Planck equation. The aerosol size distribution is compared with the experimental data. The results show that the aerosol size distribution is affected by the turbulence. The aerosol size distribution is broader than the experimental data. The aerosol size distribution is also affected by the aerosol size. The aerosol size distribution is broader for larger aerosol sizes. The aerosol size distribution is also affected by the turbulence intensity. The aerosol size distribution is broader for higher turbulence intensity. The aerosol size distribution is also affected by the aerosol size and turbulence intensity. The aerosol size distribution is broader for larger aerosol sizes and higher turbulence intensity.

© 2007 Elsevier Ltd. All rights reserved.

PACS: 02.30.Z; 42.68.J; 42.68.W; 92.60.M; 84.40.X; 02.60.P

Keywords: Aerosol; Turbulence; Dynamics; Fokker-Planck equation; Langevin equation; Gravitational settling

### 1. Introduction

In a turbulent flow, the aerosol motion is affected by the turbulence. The aerosol motion is described by the Langevin equation. The aerosol size distribution is calculated by the Fokker-Planck equation. The aerosol size distribution is compared with the experimental data. The results show that the aerosol size distribution is affected by the turbulence. The aerosol size distribution is broader than the experimental data. The aerosol size distribution is also affected by the aerosol size. The aerosol size distribution is broader for larger aerosol sizes. The aerosol size distribution is also affected by the turbulence intensity. The aerosol size distribution is broader for higher turbulence intensity. The aerosol size distribution is also affected by the aerosol size and turbulence intensity. The aerosol size distribution is broader for larger aerosol sizes and higher turbulence intensity.

$$\tau_r(\lambda) = \int_0^\infty \pi r^2 Q(r, \lambda, \eta) n(r) r + \varrho(\lambda), \quad (1)$$

where  $\tau_r$  is the aerosol size distribution;  $n(r)$  is the aerosol size distribution;  $Q(r, \lambda, \eta)$  is the aerosol size distribution;  $\varrho(\lambda)$  is the aerosol size distribution;  $\eta$  is the aerosol size distribution.

\*Tel.: +86 10 8299 8132; fax: +86 10 6201 0846.

E-mail address: [yw@igge.cma.gov.cn](mailto:yw@igge.cma.gov.cn)



$$Pr = \frac{\dot{y}}{r} \left( \frac{r}{r_0} \right)^{2n} \frac{H}{n(y)} \quad (2) \quad w = \frac{r}{r_0} \quad o_i$$

$d_i$

... I W ... , n(r) ... ( ... , ... , ... ) ...  
 ... T ... ) ... T ...  
 ... T ... ) ... T ...  
 ... U ... , W ...  
 ...

$$M(n) := \frac{1}{2} \|Kn - d\|^2 \dots - H(n) \leq \Delta_1, \|Ln\|^2 \leq \Delta_2, 0 \leq n < \infty, \tag{10}$$

... L ... S ... W<sup>1,2</sup> ... n(r), w ... ( W ... , 2006 ...  
 ... ) ... E ... (10) ... ; ... E ...  
 (10) ... T ... E ... (10) ...  
 ... (W ... , 2007; W ... & Y ... , 2005; Y ... , 1993). W ...  
 S ... (10) ... W ...

$$\begin{aligned} \Psi(n) &:= \frac{1}{2} \|Kn - d\|^2 + v \|Ln\|^2 + \mu(-H(n)) \\ &= \frac{1}{2} \|Kn - d\|^2 + v \|Ln\|^2 + \mu \int n(r) \dots n(r) r \end{aligned} \tag{11}$$

... S = {n : n ... , r ... 0 ≤ n < ∞}, w ... v ... μ ... w ... r ...  
 W ... r ...  
 N ... r ... (11) ... r ...

$$\tilde{\Psi}(\vec{n}) := \frac{1}{2} \|\mathcal{K}\vec{n} - \vec{d}\|^2$$

3.2. A gradient method for solving a regularized solution

$$g(\vec{n}) = \mathcal{K}^T(\mathcal{K}\vec{n} - \vec{d}) + \nu \mathcal{L}^T(\mathcal{L}\vec{n}) + \mu (1 + \dots (w_{\vec{n}} \cdot \vec{n})),$$

$$(1 + \dots (w_{\vec{n}} \cdot \vec{n})) := [1 + \dots (w_{n_1} \cdot n_1), 1 + \dots (w_{n_2} \cdot n_2), \dots, 1 + \dots (w_{n_p} \cdot n_p)]^T,$$

$$\vec{n}_{k+1} = \vec{n}_k + \omega_k s_k,$$

$$s_k = -g_k, g_k = g(\vec{n}_k), \omega_k = \dots (0, \|\mathcal{K}\|^{-2}),$$

$$\vec{n}_{k+1} = \vec{n}_k + \omega s_k.$$

$$s_k = g_{k+1} - g_k, s_k = \vec{n}_{k+1} - \vec{n}_k$$

$$M(\vec{n}), \dots (13).$$

$$\tilde{\Psi}_r - \tilde{\Psi}(\vec{n}_k + \beta s_k) \geq -\beta \gamma_1 s_k^T g_k. \tag{20}$$

If  $L_r > 0$ ,  $\tilde{\Psi}_r$  is a concave function of  $\vec{n}$ . Let  $\tilde{\Psi}(\vec{n}) = L_r \vec{n} + \dots$ . Then  $\tilde{\Psi}_r$  is a concave function of  $\vec{n}$ . (Wang & M, 2007) (Dunn & Frazee, 2003; Marrero & Tardieu, 1991) :

$$\|\tilde{g}_k\|_2 \leq \varepsilon \|g_1\|_2, \tag{21}$$

where  $\tilde{g}_k$  is defined as

$$(\tilde{g}_k)_i = \begin{cases} (g_k)_i & (\vec{n}_k)_i > 0, \\ \{(g_k)_i, 0\} & (\vec{n}_k)_i = 0. \end{cases}$$

Now, we can describe the BB method for maximum entropy regularization:

**Algorithm 3.1** (BB method for maximum entropy regularization).

- Step 1: Initialize  $\vec{n}_0$ ,  $\varepsilon > 0$ ,  $k := 1$ .
- Step 2: Compute  $\tilde{\Psi}_r$  and  $\tilde{\Psi}(\vec{n}_k)$  using (21);  $O(n^2)$ ,  $s_k = -g_k$ .
- Step 3: If  $k = 1$ ,  $\alpha_k = W$  (17) (18). Otherwise,  $\alpha_k = \alpha_k^{BB1}$  or  $\alpha_k^{BB2}$ .
- Step 4: Update  $\vec{n}_{k+1} = \vec{n}_k + \alpha_k s_k$ .
- Step 5: Evaluate  $\tilde{\Psi}_r$  and  $\tilde{\Psi}(\vec{n}_{k+1})$  using (20) and (21);  $O(n^2)$ ,  $s_{k+1} = -g_{k+1}$ .
- Step 6: Normalize  $\tilde{\Psi}_r$  and  $\tilde{\Psi}(\vec{n}_{k+1})$  using (3.2);  $O(n^2)$ .

$$\vec{n}_{k+1} = \vec{n}_k + \beta s_k, \quad s_{k+1} = -g_{k+1}.$$

Step 7: Let  $k := k + 1$  and go to Step 2.

Since  $\tilde{\Psi}_r$  is a concave function of  $\vec{n}$ , we have  $\tilde{\Psi}_r(\vec{n}_k) \geq \tilde{\Psi}_r(\vec{n}_{k+1})$ . If  $\tilde{\Psi}_r(\vec{n}_k) = \tilde{\Psi}_r(\vec{n}_{k+1})$ , then  $\tilde{\Psi}_r$  is constant on the line segment between  $\vec{n}_k$  and  $\vec{n}_{k+1}$ . Otherwise,  $\tilde{\Psi}_r(\vec{n}_k) > \tilde{\Psi}_r(\vec{n}_{k+1})$ . Then  $\tilde{\Psi}_r$  is a concave function of  $\vec{n}$ . (3.2)

**Algorithm 3.2** (Nonmonotone line search).

- Step 1: Given  $L_r > 0$ ,  $\tilde{\Psi}_r$ ,  $\tilde{\Psi}(\vec{n}_k)$ ,  $\tilde{\Psi}_r = \infty$ .
- Step 2: A line search for  $\tilde{\Psi}_r$ :
  - If  $\tilde{\Psi}_r(\vec{n}_k) < \tilde{\Psi}_r$ ,  $\tilde{\Psi}_r := \tilde{\Psi}_r(\vec{n}_k)$ ,  $l := 0$ .
  - Otherwise,  $\tilde{\Psi}_r := \{\tilde{\Psi}_r, \tilde{\Psi}_r(\vec{n}_k)\}$ ,  $l := l + 1$ . If  $l = L$ ,  $\tilde{\Psi}_r := \tilde{\Psi}_r$ ,  $\tilde{\Psi}_r := \tilde{\Psi}_r(\vec{n}_k)$ ,  $l := 0$ .
  - Update  $\tilde{\Psi}_r$  using (20).

3.3. Aerosol particle size distribution function retrieval

$$n(r), w \in [0.1, 10] \mu\text{m}, N \tag{6}$$

$(N \leq 20)$ ,  $N = 200$ .

(1978),  $h(r) = f(r) = n(r) = h(r)f(r)$ ,  $h(r) = \int_a^b [k(r, \lambda, \eta)h(r)]f(r) dr$ ,  $h(r) = r^{-(\nu^*+1)}$ ,  $\nu^* = 3.0$ .

$$\tau_r(\lambda) = \int_a^b [k(r, \lambda, \eta)h(r)]f(r) dr, \tag{22}$$

$$k(r, \lambda, \eta) = \pi r^2 Q(r, \lambda, \eta) k(r, \lambda, \eta)h(r), \quad (\mathcal{E}f)(\lambda) = \tau_r(\lambda). \tag{23}$$

$$\frac{1}{2} \|\mathcal{H}\vec{f} - \vec{\tau}_r\|^2 + \nu \|\mathcal{L}\vec{f}\|^2 + \mu \sum_i f_i (w_{f_i} \cdot f_i), \tag{24}$$

$$w_{\vec{f}} := [w_{f_1}, w_{f_2}, \dots]^T, \quad e^{\mathcal{T}\vec{f}} \cdot \mathcal{H}\vec{f} = \vec{\tau}_r, \quad \vec{f} \geq 0 \tag{25}$$

$\{\vec{f} : \mathcal{H}\vec{f} = \vec{\tau}_r, \vec{f} \geq 0\}$ ,  $w_{\vec{f}} = e^{\mathcal{T}\vec{f}} \cdot \mathcal{H}\vec{f}$ ,  $\mu_k = \mu_0 \cdot \xi^{k-1}$ ,  $0 < \xi < 1$ ,  $\mu_0 = 0.5$ ,  $k = 1, 2, \dots$

$$\mu_k = \mu_0 \cdot \xi^{k-1}, \quad 0 < \xi < 1, \tag{26}$$

$\mu_0 \in (0, 1)$ ,  $\mu_k = 0.5$ ,  $k = 1, 2, \dots$

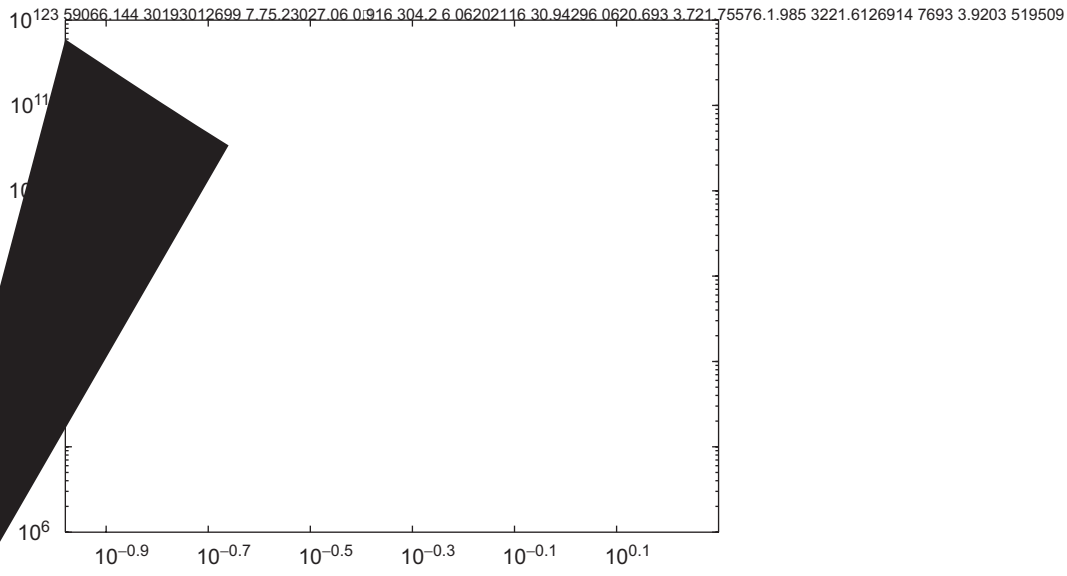
**4. Numerical experiments**

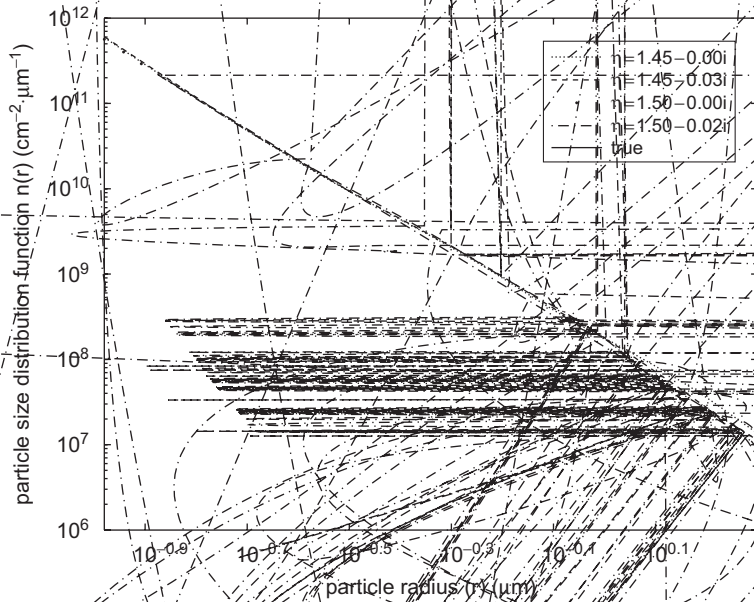
*4.1. Theoretical simulation*

$\mathcal{H}\vec{f} = \vec{\tau}_r$ ,  $\mathcal{L}\vec{f} = \vec{0}$ ,  $\mu_k = \mu_0 \cdot \xi^{k-1}$ ,  $0 < \xi < 1$ ,  $\mu_0 = 0.5$ ,  $k = 1, 2, \dots$

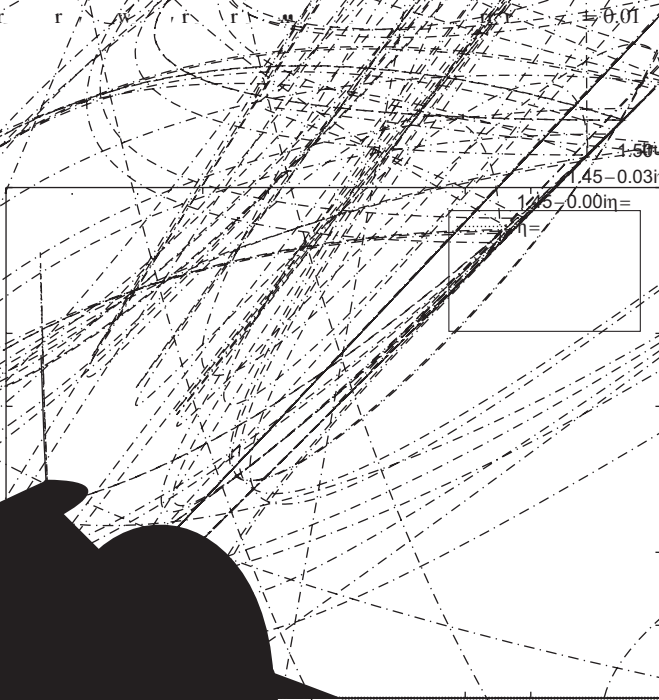








F. 3. L



F. 4. L

$\delta = 0.01$   
 $\frac{2}{2} = 0.036$   
 $f_{\infty}(r) w$   
 $1.45 - 0.00, 1.45 - 0.03, 1.50 - 0.00$   
 $N_{\infty}(r)$

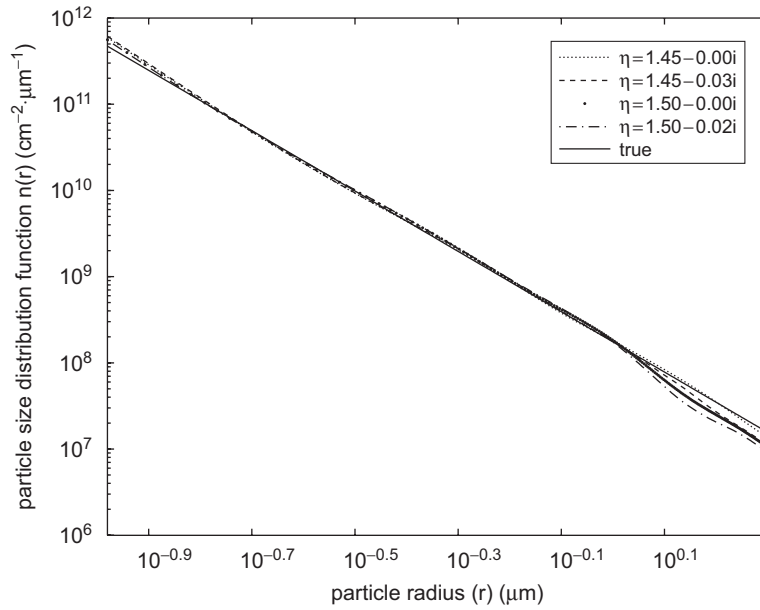


Fig. 5. Log-log plot of particle size distribution function  $n(r)$  versus particle radius  $r$  for  $\delta = 0.05$ .

Table 1  
Comparison of numerical results for  $\delta = 0.005, 0.01, 0.05$ .

$N$	$\eta = 1.45 - 0.00i$	$\eta = 1.45 - 0.03i$	$\eta = 1.50 - 0.00i$	$\eta = 1.50 - 0.02i$
$\delta = 0.005$	$1.4501 \times 10^{-4}$	$8.7595 \times 10^{-5}$	$9.8996 \times 10^{-5}$	$1.0632 \times 10^{-4}$
$\delta = 0.01$	$1.5067 \times 10^{-4}$	$9.2079 \times 10^{-5}$	$6.8340 \times 10^{-5}$	$1.0414 \times 10^{-4}$
$\delta = 0.05$	$3.1027 \times 10^{-4}$	$2.5333 \times 10^{-4}$	$1.8165 \times 10^{-4}$	$2.1722 \times 10^{-4}$

Table 2  
Comparison of numerical results for  $\delta = 0.005, 0.01, 0.05$  (CPU time in parentheses).

$N$	$\eta = 1.45 - 0.00i$	$\eta = 1.45 - 0.03i$	$\eta = 1.50 - 0.00i$	$\eta = 1.50 - 0.02i$
$\delta = 0.005$	1995 (2.8130 s)	1492 (2.1400 s)	1130 (1.6090 s)	1133 (1.4060 s)
$\delta = 0.01$	1311 (1.8900 s)	1575 (2.5940 s)	781 (1.0630 s)	1102 (1.6880 s)
$\delta = 0.05$	1348 (1.9210 s)	2000 (2.8590 s)	1329 (1.5470 s)	894 (1.2810 s)

Fig. 8, 9. Comparison of numerical results for  $\delta = 0.005, 0.01, 0.05$  with the true solution. The x-axis is particle radius  $r$  ( $\mu\text{m}$ ) and the y-axis is particle size distribution function  $n(r)$  ( $\text{cm}^{-2} \mu\text{m}^{-1}$ ). The true solution is shown as a solid line, and the numerical results are shown as dotted, dashed, dash-dot, and long-dashed lines for different values of  $\eta$ .

#### 4.2. Discussions on numerical results

In this paper, we have presented a numerical method for solving the particle size distribution function  $n(r)$  for a given set of parameters. The method is based on the CE 318 (Chen et al., 2006) and is implemented in the software package *Wang et al. (2006)*.

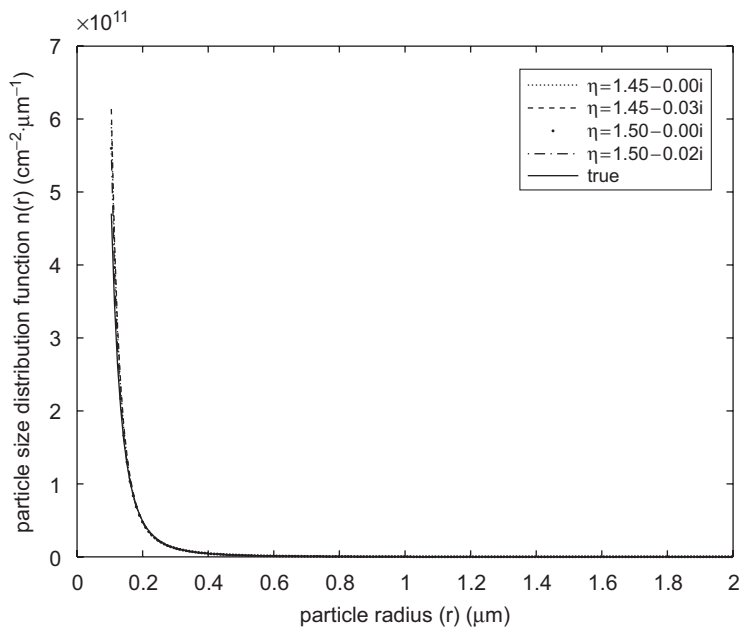


Fig. 6. Particle size distribution function  $n(r)$  vs particle radius  $r$  for  $\delta = 0.05$ .

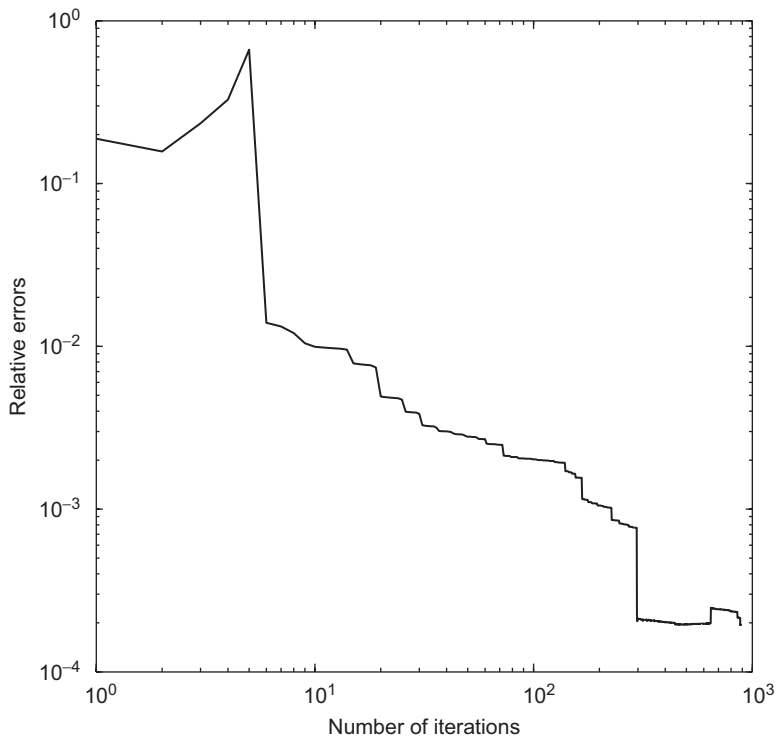


Fig. 7. Number of iterations vs relative errors.



F. 108

10

10

10

aerosol particle radius ( $\mu$ )



where  $y_k = g_{k+1} - g_k$ ,  $s_k = x_{k+1} - x_k$ .  $R = A^{-1}y$  ( $\alpha > 0$ )

$$\|y_{k-1} - \alpha^{-1}Is_{k-1}\|^2$$

$y$

$$\alpha_k^{BB1} = \frac{s_{k-1}^T s_{k-1}}{s_{k-1}^T y_{k-1}} \tag{A.4}$$

where  $y = \alpha I s_{k-1} - s_{k-1}$ ,  $A = \alpha I - A$ ,  $w = \alpha_k$

$$\|\alpha I y_{k-1} - s_{k-1}\|^2$$

$$\alpha_k^{BB2} = \frac{s_{k-1}^T y_{k-1}}{y_{k-1}^T y_{k-1}} \tag{A.5}$$

where  $s_{k-1} = -\alpha_{k-1}g_{k-1}$ ,  $y_{k-1} = As_{k-1}$ ,  $w = \alpha_k$ . Eqs. (A.4)–(A.5):

$$\alpha_k^{BB1'} = \frac{g_{k-1}^T g_{k-1}}{g_{k-1}^T A g_{k-1}} \tag{A.6}$$

$\alpha g$



Step 3:  $C_{k+1} := b_{k+1}$  (B.2)  $\beta_k$ ;  $O_{k+1} := \alpha_k$ ,  $b_{k+1} := b_k$ . If  $b_{k+1} < +\infty$ , Step 4:  $C_{k+1} := (a_{k+1} + b_{k+1})/2$ ,  $k := k + 1$ .

$\lambda_1 = 1.0 \times 10^{-4}$ ,  $\lambda_2 = 0.9$ .  
*BB subroutine:*  $\vec{n}_{k+1} = \vec{n}_k + s_k$ .  $\alpha_k^{BB1} = \alpha_k^{BB2}$  (A.4),  $\alpha_k^{BB} = \alpha_k^{BB1}$  (A.5).  $\alpha_k^{BB1}$ ,  $\alpha_k^{BB2}$ ,  $\alpha_k^{BB}$  are nonmonotone subroutines.  $\alpha_k^{BB1} = \alpha_k^{BB2}$  (A.7),  $\alpha_k^{BB2}$  is a  $W^{1,2}$  function.

**References**

Åstrand, A. (1929). *Geografiska Annaler*, 11, 156–166.  
 Briggs, J., & Brackley, J. (1988). *IMA Journal of Numerical Analysis*, 8, 141–148.  
 Brackley, J., & C. (2001). *Applied Optics*, 40, 1329–1342.  
 Briggs, J., & Kruger, A. (2006). *Computer Physics Communications*, 174, 607–615.  
 Bracewell, R. N., & H. (1983). *Absorption and scattering of light by small particles*. New York: Wiley.  
 Chou, M. T. (1970). *Journal of Aerosol Science*, 27, 960–967.  
 Dong, Y. H., & Farin, R. (2003). *Projected Barzilai–Borwein methods for large-scale box-constrained quadratic programming*. University of Delaware, Report NA/215.  
 Dong, C. N. (1974). *Journal of Aerosol Science*, 5, 293–300.  
 Engl, H. W., Hanke, M., & Neubauer, A. (2000). *Regularization of inverse problems*. Dordrecht: Kluwer Academic Publishers.  
 Farin, R., Brackley, J., & P. (1995). *Applied Optics*, 34, 5829–5839.  
 Farin, R. (2001). *On the Barzilai–Borwein method*. University of Delaware, Report NA/207.  
 Griggs, H. (1971). *Applied Optics*, 10, 2534–2538.  
 Hansen, J. T., Morfitt, L. G., Collins, B. A., Hansen, N., Keeling, A., & Munnich, K. (1996). *Climate change 1995*. Cambridge: Cambridge University Press.  
 Jongschaap, E. T. (1968). *IEEE Transactions on Systems Science and Cybernetics, SSC-4*, 227–241.  
 Johnson, C. E. (1955). *Journal of Meteorology*, 12, 13–25.  
 Keeling, M. D., Byrd, D. M., Hansen, B. M., & Ramanamirtham, J. A. (1978). *Journal of Aerosol Science*, 35, 2153–2167.  
 Leung, K., & R. (1994). *The Astrophysical Journal*, 425, 653–667.  
 Mather, G. J. (1976). *Optics of atmosphere*. New York: Wiley.  
 Moré, J., & Toraldo, G. (1991). *SIAM Journal on Optimization*, 1, 93–113.  
 Powell, D. L. (1962). *Journal of the Association for Computing Machinery*, 9, 84–97.  
 Szwed, G. E. (1979). *Applied Optics*, 18, 988–993.  
 Sun, K. S., & Zeng, L. G. (1996). *Applied Optics*, 35, 2114–2124.  
 Tautou, A. N., & Aronov, V. Y. (1977). *Solutions of ill-posed problems*. New York: Wiley.  
 Tardif, P. L. (1997). *Mathematical Programming*, 77, 69–94.  
 Twiss, S. (1963). *Journal of the Association for Computing Machinery*, 10, 97–101.  
 Twiss, S. (1975). *Journal of Computational Physics*, 18, 188–200.  
 Twiss, S. (1977). *Atmospheric aerosols*. Amsterdam: Elsevier.  
 Verma, A., & Keeling, J. P. (2000). *Journal of Aerosol Science*, 31(Suppl. 1), 767–768.  
 Wang, Y. F. (2007). *Computational methods for inverse problems and their applications*. Beijing: Higher Education Press.  
 Wang, Y. F., Fu, S. F., & Fu, X. (2007). *Journal of Aerosol Science*, 38, 885–901.  
 Wang, Y. F., Fu, S. F., Fu, X., Yang, G. J., & Gong, Y. N. (2006). *Applied Optics*, 45, 7456–7467.

Wang, Y. F., & Miao, S. Q. (2007). Parameter estimation of aerosol particle size distribution by using the multi-angle light scattering. *Inverse Problems in Science and Engineering*, 15(6), 559–583.

Wang, Y. F., & Yu, Y. X. (2005). Characterization of aerosol particle size distribution by using the multi-angle light scattering. *Inverse Problems*, 21, 821–838.

Wang, D. L. (2000). Retrieval of aerosol optical properties from multi-angle light scattering measurements. *Journal of Aerosol Science*, 31, 1–18.

Wang, D. L., Yu, S. C., Kulkarni, P. S., McGraw, R., Swerdlow, S. E., Sato, V. K., et al. (2002). Retrieval of aerosol optical properties from multi-angle light scattering measurements. *Journal of Aerosol Science*, 33, 319–337.

Xu, T. Y., Yu, S. G., & Wang, Y. F. (2003). *Numerical methods for the solution of inverse problems*. Beijing: Science Press.

Yeh, G., & Tatarski, M. (1969). Diffraction of light by a random distribution of spheres. *Applied Optics*, 8, 447–453.

Yu, Y. X. (1993). *Numerical methods for nonlinear programming*. Shanghai: Shanghai Scientific Technical Publishers.

Yu, Y. X., & Sun, W. Y. (1997). *Theory and methods of optimization*. Beijing: Science Press.